4 RESULTS

All the results presented were obtained during the present research.

4.1 GEOGRAPHICAL INFORMATION SYSTEM (GIS).

The primary reason for using a GIS was to make the gathered data easier to access and to present it to as wide an audience and user community as possible. The GIS software used during the investigation is Arcview 3.1(ESRI, 1998). The digitized contours were used to create a digital terrain model (Figure 12). The GIS was used as a data base and mapping tool with limited interpretation. General information such as contours, drainage channels, access roads, etc. were digitised forming the base data to work from (Table 3). All the linear features mapped were also captured on the GIS.

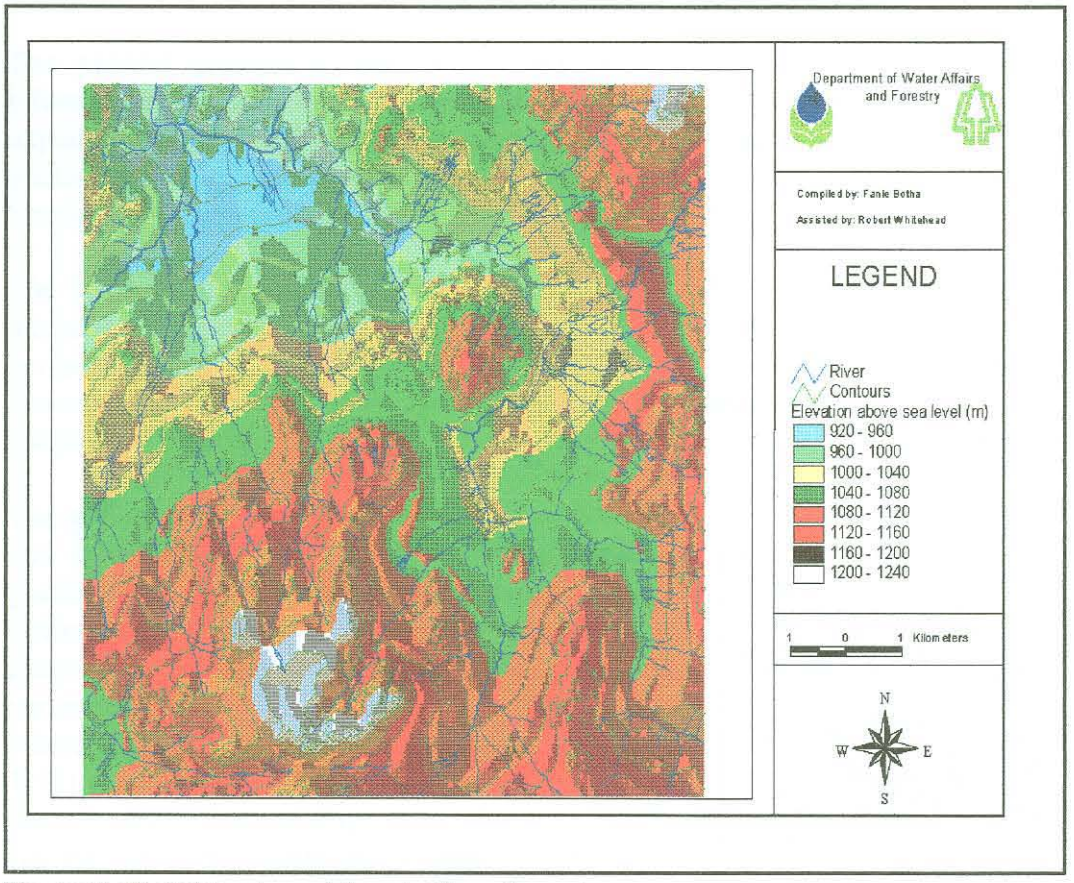

Figure 12. Digital terrain model created from the contours.

The different data layers in the GIS were also used for querying purposes to select new drilling sites.

Table 3.GIS information captured.

Name/Item	Scale/Source	Actions
Contours	1: 10 000	Digitise 20 metre contours from ortho-photos.
Rivers	1 : 10 000	Digitise rivers from ortho-photos.
Villages	[4]NGDB	Copy data from available data.
Topo sheets	1 : 50 000	Data from 1:50 000 toposheets.
Geology	[5]CGS	Data from 1: 250 000 2428 Nylstroom Sheet.
Regional Structures	[6]BOSGIS	Copy data from existing data.
Joints and Faults	1 : 10 000	Digitise linear features and map in field
Current boreholes	GPS	Capture data in the field with GPS
New boreholes	GPS	Capture data in the field with GPS

4.2 GENERAL GEOLOGY

The general geology is important in any ground water investigation. Geological information is readily available as published 1:250 000 sheets with an accompanying explanatory booklet. Both, the published 1 : 250 000 geological map and the field geological map of the research area were consulted (Figure 13). Handbook no. 8 of the Stratigraphy of South Africa (SACS, 1980) provide most of the necessary information.

The Nebo Granite forms part of the Lebowa Granite Suite, which is part of the later intrusive stages of the Bushveld Igneous Complex. The Nebo Granite is a plate like intrusion resting on the Rustenburg Layered Suite (RLS), with the contact dipping 5°to the north northwest. The thickness of the intrusion varies from 420m in the south to 2400m in the north.

The granite has a medium to coarse grained texture and its mineralogy is typically quartz, plagioclase, perthite, hornblend and/or biotite (Frame 4). At the bottom of the intrusion the anorthite content in the plagioclase increases from 12% to 20%. The colour varies from a grey white at the base to a pinkish colour where the mafic minerals become less prominent (4-11%). At the base of the intrusion there may be breccia present consisting of huge rugged norite blocks, representing the magma influx pipe. The Klipkloof Granite also forms part of the Lebowa Granite Suite. This is a medium to fine grained granite, occurring as porphyritic dykes or sills.

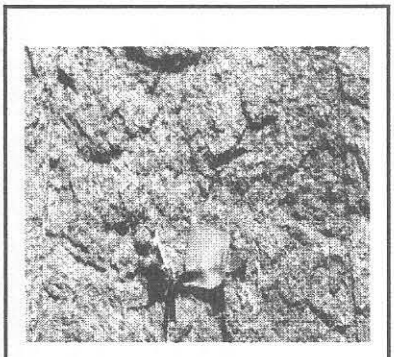

Frame 4 Typical Nebo Granite.

[4] NGDB - National Ground water Data Base, DWAF.

[5]CGS -Council for Geoscience.

[6]BOSGIS - Bushveld Igneous Complex Geographical Information System.

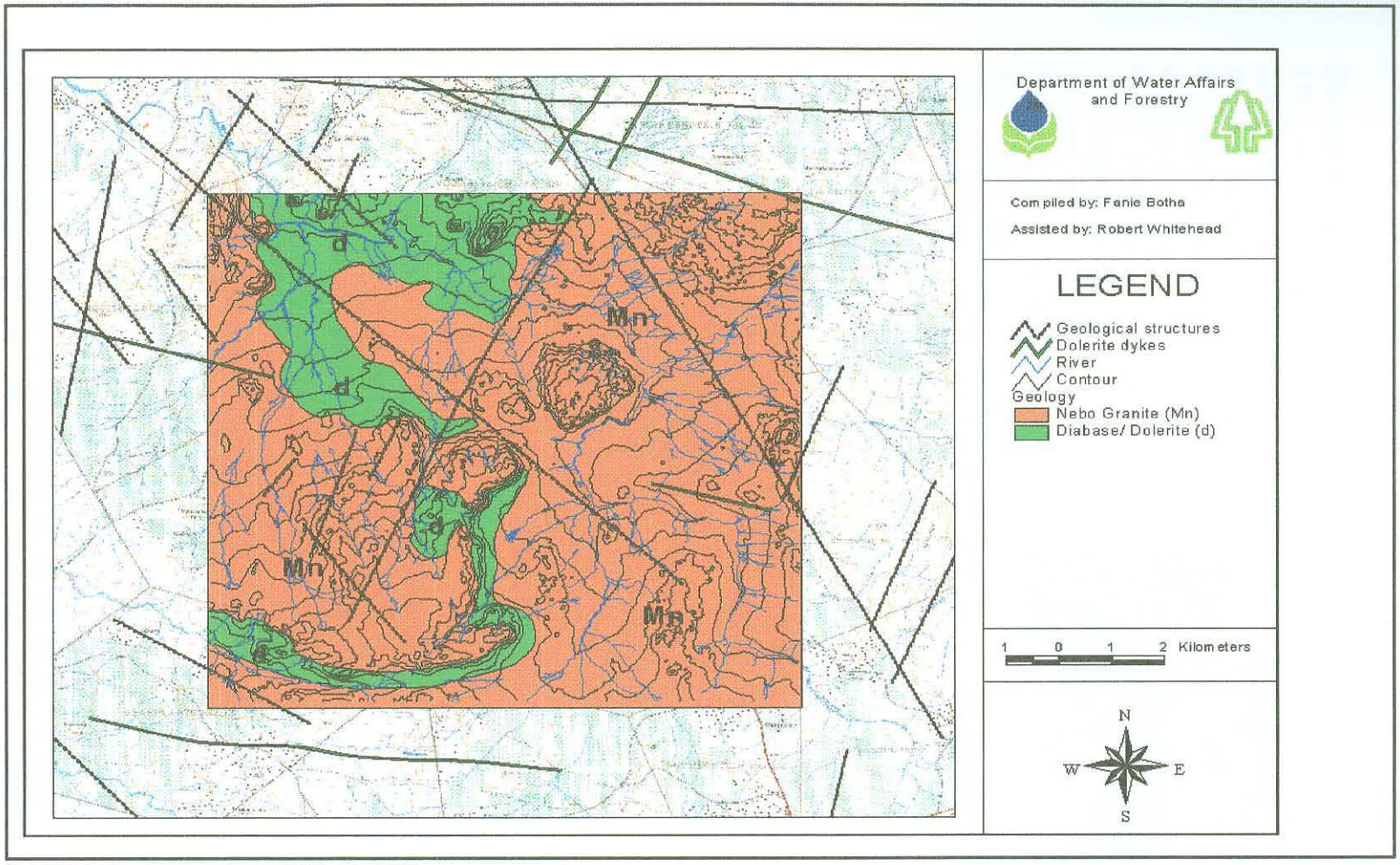

Figure 13. General geology and geological structures obtained from the 1: 250 000 Nylstroom geological sheet

The Klipkloof Granite is more prominent in the southern part of the Nebo Granite.

The Nebo Granite outcrop is surrounded by younger Karoo basaltic rocks in the west, which form the flat lying Springbok Flats with the Transvaal sediments in the north and rocks from the Rustenburg Layered Suite in the east.

Dolerite dykes, striking 20° - 30° and 110° – 130° of Karoo Age, occur throughout the area. Some of the dykes may be followed for several tens of kilometres through the Lebowa Granite and into the Rustenburg Layered Suite (RLS). The dykes are often associated with fractures and are prominent in the northern part of the Nebo Granite (Figure 13). In the study area a plate like doleritic intrusion occurs and dips towards the north-west. The contact between the granite and the dolerite is quite sharp(Frame 5).

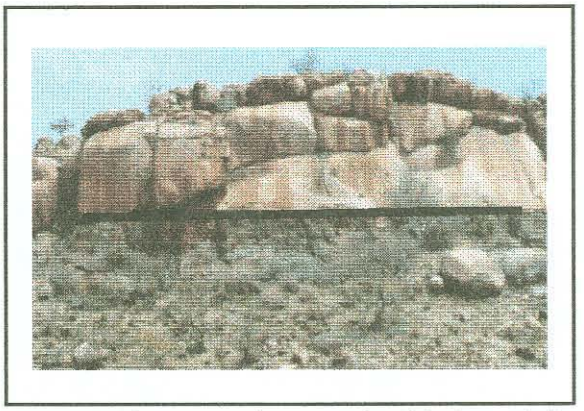

Frame 5. The contact between the dolerite and the granite.

The geological environment, as described above, consists of a fairly uniform intrusive, granitic body, which can be described as being a hard crystalline fractured rock aquifer. These aquifers are notorious for their low ground water potential and difficult ground water exploration conditions.

4.3 GEOLOGICAL STRUCTURES

4.3.1 Structural setting

The ***Wonderkop Fault*** is the most prominent regional geological structure in the area. Intersecting the granite in the west, the Olifants River follows the fault, which extends into the Rustenburg Layered Suite, to the east. The Wonderkop Fault is a strike-slip fault and indications are that the fault extends beyond the dolomite of the Chuniespoort Group to the north-east (Schwellnus, Engelbrecht, Coertzee,Russel, Malherbe, Van Rooyen Crooke, 1962). The **Steelpoort Fault** and **Sekhukhune Fault** are manifestations of two other major geological events which influenced the Lebowa Granite Suite.

Odgers and du Plessis(1989) did a regional seismic survey in the north-eastern Bushveld Complex and postulated that the occurrence of the Wonderkop Fault and the ***Malope Dome*** in such close proximity are no coincidence (Frame 6). They found that the overburden thickness varies across the fault and estimate the material under the Malope Dome could have been less dense than the surrounding material making the material buoyant. The catalyst effect of the buoyant sub-layer under the dense overburden may have promoted diapirism. The rising diapir in turn induced further variation in the overburden and consequently induced further faulting in the overburden. The composition of the rising diapir (Malope Dome) is still not certain, but gravity surveys suggest that it

is capped with a relatively thin layer of Transvaal rocks and RLS with the main body consisting of material similar to the Nebo Granite.

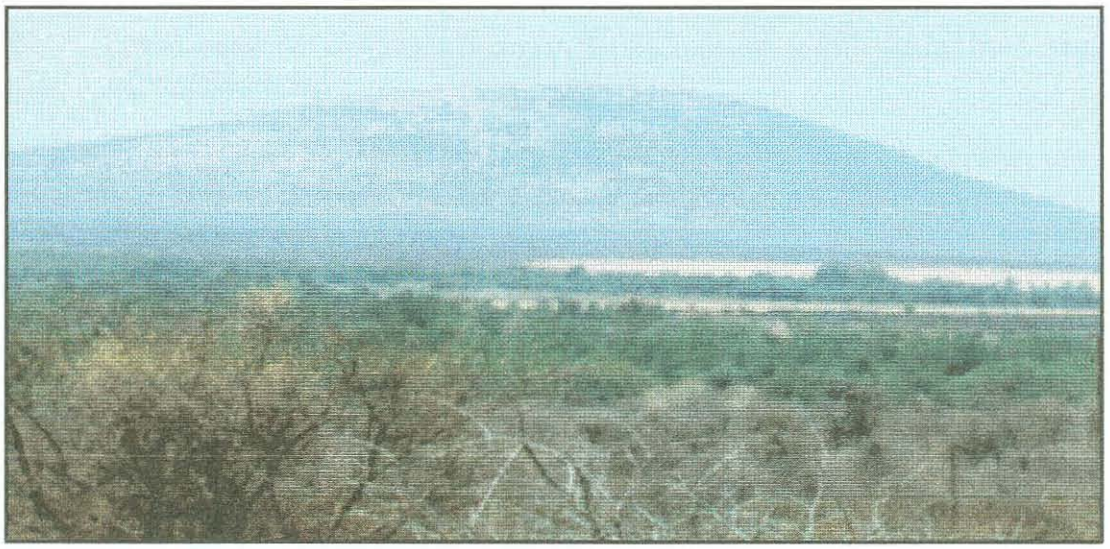

Frame 6. The Malope Dome seen from the north.

4.3.2 Structure census and mapping

The structural investigation was conducted as an honours project (Hoffmann, 1997) in the Department of Earth Science, University of Pretoria. All visible and accessible lineaments were recorded from available data, e.g. air photos and LandSat imagery, followed by field mapping. Hoffmann (1997) made the following deductions:

1. Genetically different fractures occur in the Nebo Granites, namely:
   - Cooling fractures.
   - Shear zone fractures (Faulting).
   - Quartz rich fractures due to hydrothermal activity (Intrusion).

2. Movement along discontinuities was right lateral in most cases (Frame 7).

3. Minerals are broken, rather than torn apart, making it a brittle, rather than plastic deformation. According to Davis and Reynolds (1996) brittle shearing takes place in the upper 5 -10 km of the crust and is dominated by a breaking and shearing action.

4. The joints and fractures are slightly more weathered (evident from outcrop).

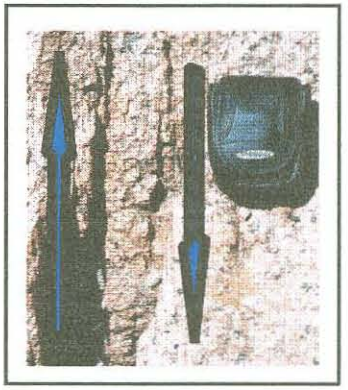

Frame 7. Typical movement along shear axes.

5. Fine grained dolerite intrusions show some of the same joint patterns as in the granite. This indicate tectonic activity younger than Karoo times.

6. Tension cracks, due to the cooling of the granite body are not prominent.

7. Discolouration of the granite occurs in the fracture zones with shades from cream red to darkish red.

From the field mapping a structural map was compiled, indicating most of the major joints occurring in the different outcrop areas. Included on this map are linear features derived from air photo interpretation. These mapped lineaments were also included as a data coverage in the GIS (Figure 14).

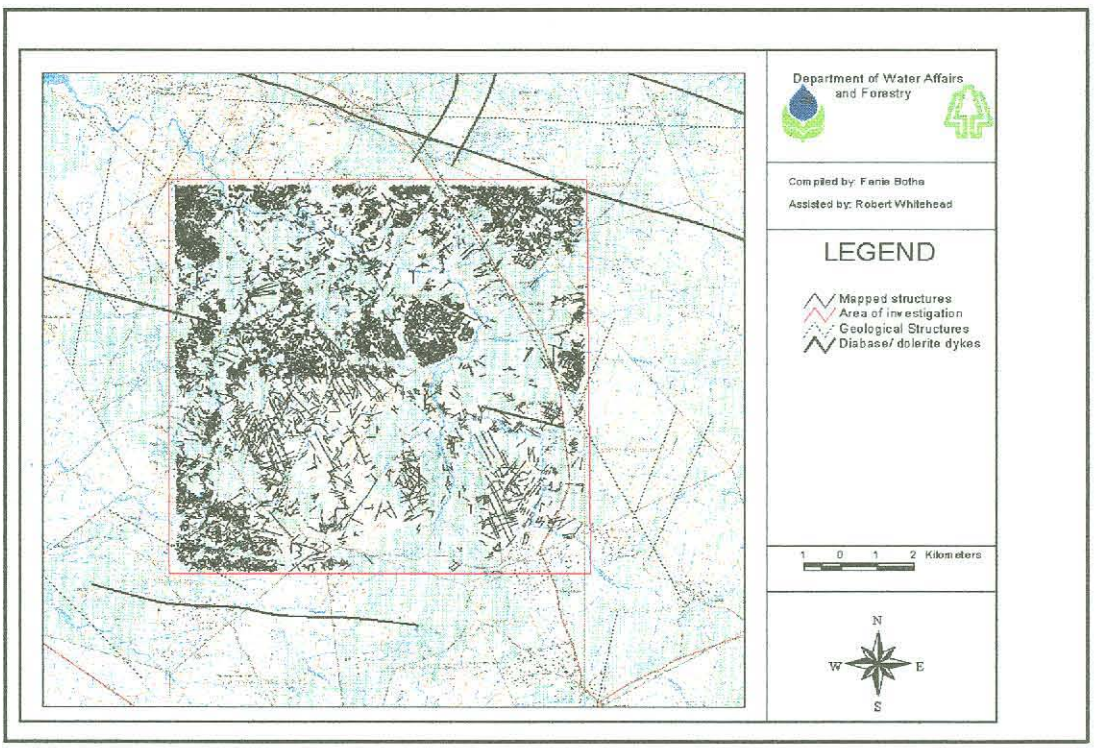

Figure 14. Linear features mapped.

4.3.3 Genetic growth and age

The objective of the structural investigation was to gather information on the nature and orientation of the most prominent geological structures. Geological structures are usually obvious targets in a ground water exploration programme in hard rock bodies.

Discontinuities in the Nebo Granite are quite prominent in rock outcrop areas. Both joint and fracture orientations can be measured with closely spaced joints occurring in fracture zones. This is thought to render the shear zone more permeable and susceptible to weathering. Prominent fractures can be followed for several kilometres using both ground surveys and aerial photographs (Frame 8).

Hoffmann (1997) investigated the major geological structures and measured a total of 761 dip and strike orientations. The data was plotted on stereo-nets from which rose diagrams were drawn. From the rose diagrams the major orientations could be calculated and captured on the GIS (Figure 15). The relative ages of the shear zones could be derived using the dolerite intrusions as a time marker (Table 4).

Frame 8. Linear lineaments can be followed for several kilometres.

Table 4. Fracture strike orientation (after Hoffmann, 1997).

	A 40° - 50°	B 80°-90°	C 120°-130°	D 140°-150°	E 170°-180°
Above dolerite	YES	YES	YES	YES	YES
In the dolerite	YES 60° -70°	YES	YES	YES	NO
Below dolerite	NO	YES	YES 110° - 120°	NO	YES

From the data (Table 4) it can be speculated that three different structural geological time intervals exist. These time intervals can be divided into the granite occurring to the north of the dolerite intrusion, the dolerite intrusion and the granite south of the dolerite intrusion (Figure 14). Some strike orientations were observed in all three geological environments while others only occur to the north of the dolerite body or below or within the dolerite.

Genetic growth of structures can be estimated by, for example, analysing intersecting joints. If two joints intersect with the one being bended towards the other and eventually joining it, it can be deduced that the deformed joint is older than the undeformed one. Using the data above Hoffmann suggests that the first structural event that took place resulted in strike orientation E, followed by events leading to A&D, then B and finally C. Hoffmann does not specifically mention whether the geological events reoccurred, but it is possible that some of the faulting may have been re-activated at later stages.

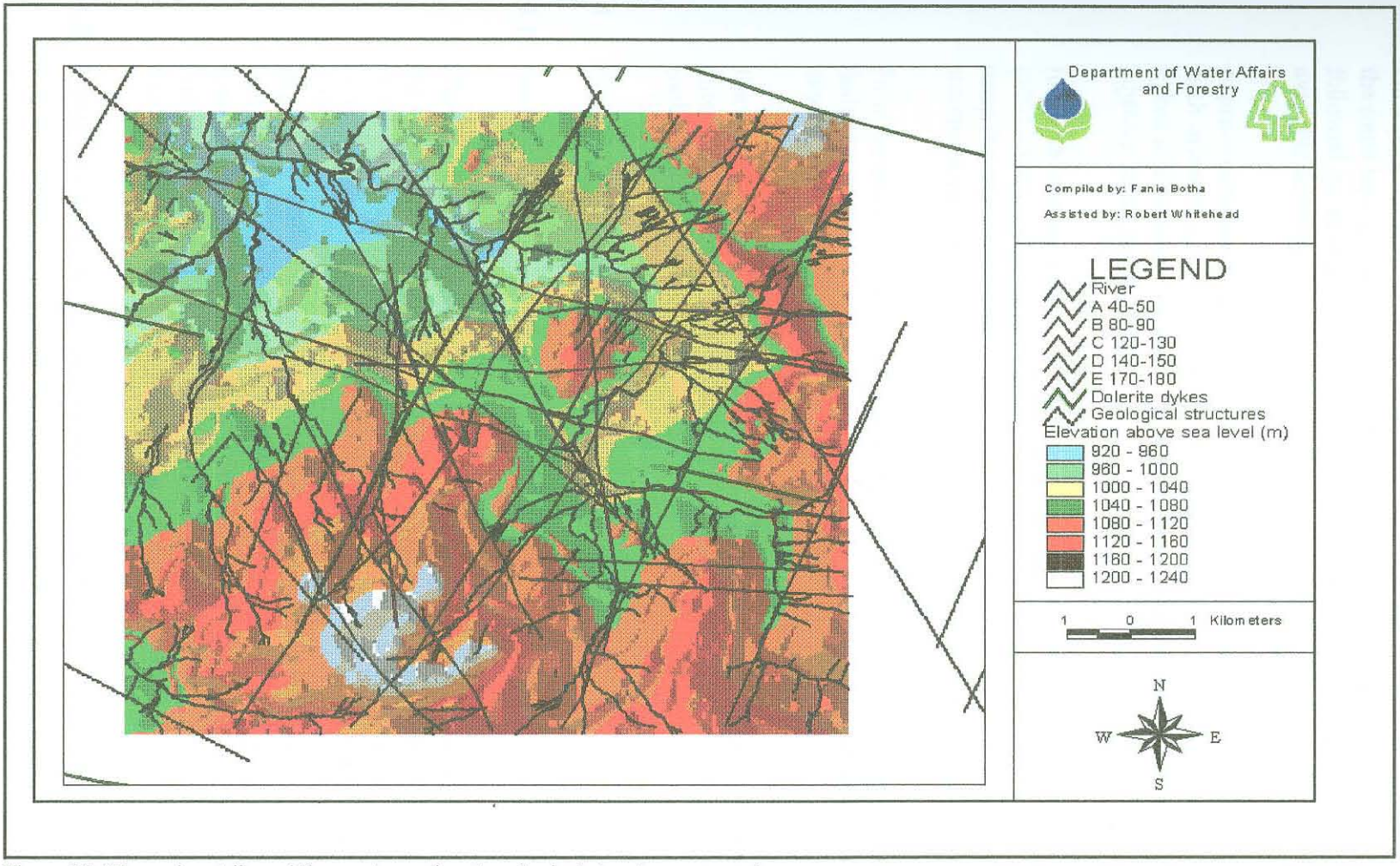

Figure 15. The major strikes of the most prominent geological structures mapped.

4.3.4 Regional setting

On a regional scale both the Wonderkop fault to the north and the Sekhukhune fault in the south have almost the same strike direction as joint set A (40° -50°). This trend is also followed by several dolerite dykes and lineaments visible from LandSat imagery and available aeromagnetic data..

A prominent geophysical lineament occurs just east of the study area and corresponds with orientation C (120° - 130°). Again this trend is followed by some of the dolerite dykes and mapped lineaments scattered across the Lebowa Granite Suite as well as in adjacent stratigraphic units.

In another study area approximately 30 km to the south, all but one strike orientation (120° - 130°) could be identified during the initial structural investigation. However, by using the experience gained during the initial study and doing more detailed surveys these structures were also found in the southern region.

From the above discussion it can be deduced that fractures and joints are associated with faulting, which corresponds with regional geological events and which in time, may be used to explain the regional tectonic history of the area.

The GIS was used to superimpose the *existing* LandSat imagery and aeromagnetic data onto the joint/fracture map. From the two data sets certain trends and major fracture zones could be identified (Figure 15).

4.4 EXISTING BOREHOLE INFORMATION

4.4.1 Borehole census

The Nebo Plateau is known for its low ground water potential with evidence supporting this fact being rather circumstantial and not based on specific research. At the time of the initial study information on the existing boreholes were obtained from the National Ground Water Data Base of the DWAF. This data was by no means complete, especially with the yield data lacking. Due to this and other constraints it was decided to conduct an independent borehole census in the research area (Table 5). Borehole positions were captured with the aid of a hand-held GPS. The captured locality points were differentially corrected using the known Telkom base station readings at Tzaneen (Table 5). The surface conditions were described and ground water levels were measured and random water samples taken for quality assessment.

4.4.2 Yields and water levels from existing boreholes

All the existing production boreholes, including those equipped with hand pumps have a static water level (S.W.L.) of less than 10 m. Boreholes were quite shallow, targeting the

deeper weathered zones rather than the fracture zones in the bedrock. Only a few of the boreholes were equipped with diesel/electricity powered mono pumps or with hand pumps being fairly common. It is therefore assumed that most boreholes had estimated yields of less than 0.5 l/s.

Table 5. Borehole census in the study area.

Borehole	Lat. (dd)	Long.	S.W.L.(m)	Borehole depth (m)	Estimated yield	Class
B01	-24.662	29.7464	N/A	N/A	0.1	B1
B02	-24.661	29.7396	N/A	84	1	C2
B03	-24.664	29.7367	N/A	N/A	0.1	B1
B04	-24.664	29.7384	4	5	0.01	A
B05	-24.6589	29.7377	N/A	N/A	0.01	A
B06	-24.6665	29.7414	4	49	0.1	B1
B07	-24.6677	29.7398	N/A	N/A	0.01	A
B08	-24.6329	29.737	N/A	N/A	1	C2
B09	-24.6213	29.7267	7	N/A	1	C2
B10	-24.6221	29.7269	7	N/A	0.1	B1
B11	-24.659	29.7	4	N/A	0.1	B2
B12	-24.5954	29.768	6	49	1	C2
B13	-24.6617	29.7475	16	24	0.1	B2
B14	-24.6613	29.748	9	N/A	0.1	B2
B15	-24.69	29.7362	7.5	65	1	C2
B16	-24.6893	29.7333	N/A	N/A	0.1	A
B17	-24.659	29.7	N/A	N/A	0.1	B2
B18	-24.6025	29.7155	N/A	N/A	0.1	B2
B19	-24.6244	29.6517	9	N/A	0.1	B2
B20	-24.6598	29.7462	14	70	0.01	A
G41170	-24.5994	29.7158	N/A	N/A	0.1	B1
G41173	-24.6032	29.7159	77	102	0.01	A
T6366	-24.6594	297371	12	63	0.01	A
T6367	-24.6594	29.7372	N/A	99	0.01	A
T6368	-24.6594	29.7377	9	63	0.01	A
T6371	-24.6658	29.7448	5	72	0.01	A
T6373	-24.6658	29.7447	N/a	90	0.01	A
T6385	-24.622	29.6583	9	58	0.1	B2
H06 0636	-24.6086	29.6638	N/A	N/A	0.1	B1

*** N/A - not available N/E - not equipped A - no pump B1 - Hand pump B2 - Hand pump out of order C1 - Diesel pump C2 - Diesel pump out of order l/s - litre per second**

4.4.3 Chemical analysis

During the initial investigation samples were taken for both inorganic and microbial analysis. Samples were analysed by Water Research Labs (PTY) Ltd of Pretoria and evaluated according to those standards accepted at the time of the investigation . The most important results from these chemical analyses were the high Nitrogen ($N0_3^-$) & Fluoride (F^-) levels. Both the average values are above the maximum allowable values for drinking water (Table 6).

Table 6. Inorganic analysis of seven existing boreholes.

Test for	Recommended value	Maximum value	Average value tested
pH	6 - 9	5.5 - 9.5	6.9
T.D.S. (mS/m*6.4)	1000	2400	663.1
Electrical conductivity (mS/m)	70	300	103.8
Ca	150	200	96.6
Na	100	400	97
Cl	250	600	139.1
N (NO_3)	6	10	*24.2*
S (SO_4)	200	600	20
Hardness (CaCO3)	300	650	308.1
F	1	1.5	*2.89*
Silica	x	x	x
Fe	0.1	1	0.45
Mn	0.05	1	0.1

*** (Recommended and Maximum values according to Weaver, 1992).**

From the organic analyses it was obvious that some kind of organic pollution takes place. Both the average total coliforms and the faecal coliform values are exponentially higher than the maximum allowable values (Table 7).

Table 7. Organic analysis of existing boreholes.

Test for	Recommended value	Maximum value	Average value tested
Total organic material (per 1000ml)	<100	1000	741.6
Total coliforms (per 100ml)	0	5	*229.67*
Faecal Coliforms. (per 100ml)	0	1	*24.67*

*** (Recommended and Maximum value according to Weaver, 1992).**

4.5 SITING OF NEW BOREHOLES

As mentioned before, the project ran parallel to a geophysical research project. Boreholes were therefore sited by using both geophysical and structural mapping results. Twenty three potentially high yielding sites were identified, of which 12 sites were selected using the structural mapping results. These sites were selected using mapping procedures as described in Chapter 3. The major geological structures and the drainage systems were superimposed on the DTM (Figure 16). From the derived map topographical lows associated with major structures could be identified. These areas were then selected as potentially high yielding sites (Figure 17). The drainage give an indication of better recharge areas.

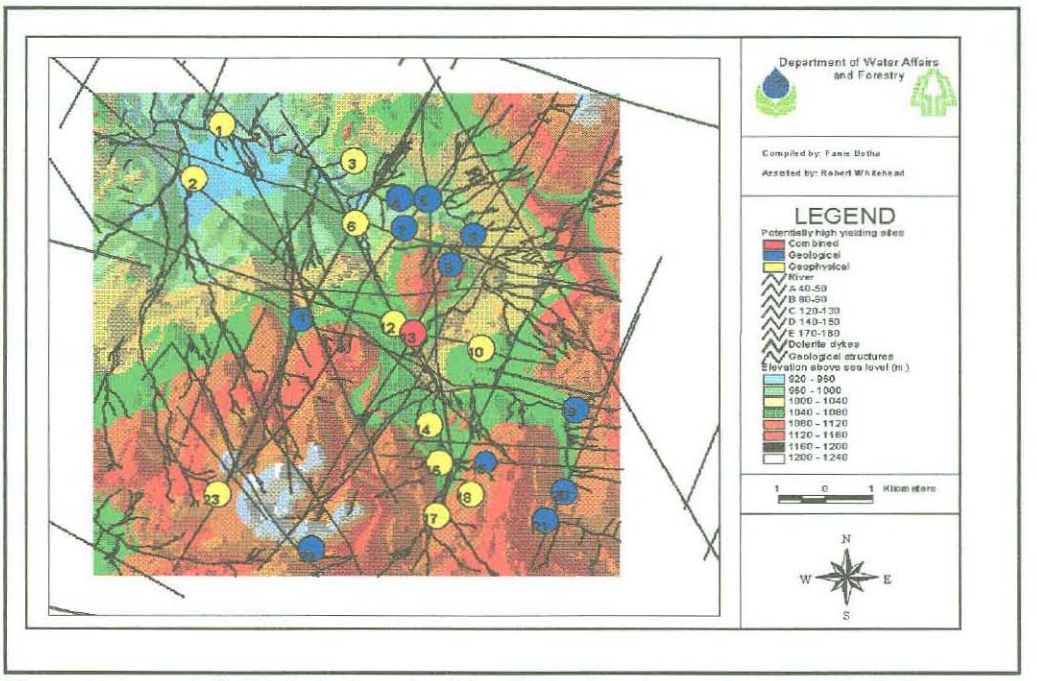

Figure 16. Potentially high yielding sites identified using structural and geophysical methods.

PHYS 1, 2, 3, 6, 10,12,13,14,15,17,18 and 23 were selected using geophysical data. The following is a summary of the 12 sites selected with the aid of structural geology.

4.5.1 Potential high yielding site no.4

This site is situated on a very prominent fracture zone with massive fracturing (Appendix 1, PHYS 4). The fracture zone can be followed in the field for several hundreds of metres. The strike of the fracture zone corresponds with strike orientation A (40° -50°).

4.5.2 Potential high yielding site no.5

PHYS 5 is also located on a well developed shear zone striking at 40°. The jointing however is not as clearly visible and the shear zone forms part of a drainage channel and most joints are covered with alluvium (Appendix 1, PHYS 5).

4.5.3 Potential high yielding site no.7

This site is located on a highly visible structure with major jointing and fracturing (Frame 9). The strike orientation again corresponds with that of strike orientation A (Appendix 1, PHYS 7).

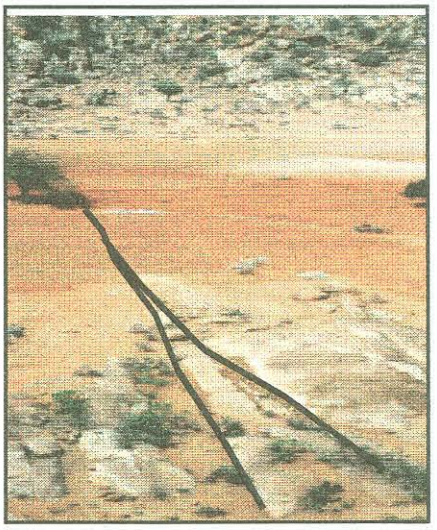

Frame 9. Linear feature at PHYS no.7

4.5.4 Potential high yielding site no.8 & 9

PHYS 8 and 9 are located on strike orientation A with clearly visible outcrops (Appendix 1, PHYS 8 & 9).

4.5.5 Potential high yielding site no.11

PHYS 11 is situated on the intersection of several structures corresponding with strike orientations A (40° - 50°), C (120° -130°) & D (140° - 150°). From the mapped data it is clear that jointing is prominent in this area (Appendix 1, PHYS 11).

4.5.6 Potential high yielding site no.13

PHYS 13 was sited using both geological and geophysical methods. In this vicinity three structures intersect A, C & D. Due to soil cover the structural approach could not pinpoint an exact position for a new borehole (Appendix 1, PHYS 13).

4.5.7 Potential high yielding site no.16

PHYS 16 was also sited on a fracture zone having the same strike orientation as A (40°-50°) (Appendix 1, PHYS 16).

4.5.8 Potential high yielding sites no.19,20 and 21

PHYS 19, 20 and 21 were all sited on fracture zones striking at 40° (Appendix 1, PHYS 19,20 & 21). Jointing and fracturing at this specific site are prominent in the field (Frame 10).

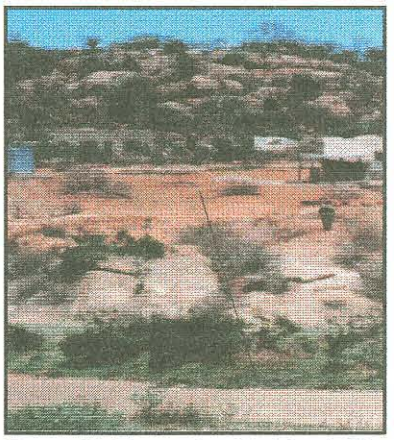

Frame 10. Fracturing highly visible at PHYS 21.

4.5.9 Potential high yielding sites no.22

PHYS 22 was positioned to drill through the dolerite sill and intersect the granite in depth. The possibility of intersecting ground water on the contact was investigated (Appendix 1, PHYS 22).